


Comparative Study of Some Numerical and Semi-analytical Methods for Some 1D and 2D Dispersive KdV-type Equations

Abey Sherif Kelil 

Nelson Mandela University, Department of Mathematics and Applied Mathematics
Gqeberha, South Africa

Received: 29 September 2021

Accepted: 10 December 2021

Abstract: This paper aims to investigate an approximate-analytical and numerical solutions for some 1D and 2D dispersive homogeneous and non-homogeneous KdV equations by employing two reliable methods namely reduced differential transform method (RDTM) and a classical finite-difference method. RDTM provides an analytical approximate solution in the form of a convergent series. The classical finite-difference method (FDM) to solve dispersive KdV equations is employed by primarily checking Von Neumann's stability criterion. The performance of the mentioned methods for the considered experiments are compared by computing absolute and relative errors at some spatial nodes at a given time; and to the best of our knowledge, the comparison between these two methods for the considered experiments is novel. Knowledge acquired will enable us to build methods for other related PDEs such as KdV-Burgers, stochastic KdV and fractional KdV-type equations.

Keywords: Dispersive KdV equations, homogeneous, non-homogeneous, reduced differential transform method, classical finite difference method.

1. Introduction

Nonlinear partial differential equations are obtained when problems in numerous domains in science and engineering are modeled. Since the discovery of solitons in 1965 by Zabusky and Kruskal [24], numerous nonlinear PDEs have been derived and extensively applied in many branches of physics and mathematics; for example, they appear in fluid mechanics, chemical kinetics, plasma physics, nonlinear optics, condensed matter, solid-state physics, the theory of turbulence, ocean dynamics, biophysics and star formation and others. The well-known Korteweg-de Vries (KdV) equation is a nonlinear dispersive partial differential equation that describes solitary water waves (also called

*Correspondence: abey@aims.ac.za

2020 *AMS Mathematics Subject Classification:* 34A45, 35A22, 35A25

This article is licensed under a Creative Commons Attribution 4.0 International License.

Also, it has been published considering the Research and Publication Ethics. 1

solitons) in a shallow water. This equation is given by

$$u_t + \gamma uu_x + \beta u_{xxx} = 0, \quad \beta > 0, \quad (1)$$

which describes the evolution of small amplitude, long water waves down a canal of rectangular cross-section [20].

Semi-analytical methods for solving some linear as well as nonlinear partial differential equations provide approximate analytical solutions, among which we can mention Adomian decomposition method [4, 5, 22], variational iteration method [1] and homotopy perturbation method [13–15]. The authors in [3] investigated classical and multisymplectic schemes for linearized KdV equations using some numerical methods and dispersion analysis was studied. Some semi-analytic methods were also applied to study linear and nonlinear dispersive KdV equations by Appadu et al. [8, 10].

The aim of this paper is to provide a comparative study for solving 1D homogeneous and 2D non-homogeneous dispersive KdV type equations using RDTM and classical FDM for the first time in literature. The obtained solutions by these mentioned methods will be compared to confirm the reliability of the used methods.

2. Numerical Experiment

We investigate two numerical experiments, as stated below:

- (i) One-dimensional homogeneous nonlinear dispersive KdV equation [23]

$$u_t + 6uu_x + u_{xxx} = 0, \quad (2)$$

with $(x, t) \in [0, 2\pi] \times [0, 0.10)$. The initial condition is $u(x, 0) = x$ and the boundary conditions are $u(0, t) = 0$, $u_x(0, t) = \frac{1}{1+6t}$, $u_{xx}(0, t) = 0$. The exact solution is $u(x, t) = \frac{x}{1+6t}$.

- (ii) Two-dimensional dispersive non-homogeneous KdV equation given by

$$\frac{\partial u}{\partial t} + \frac{\partial^3 u}{\partial x^3} + \frac{\partial^3 u}{\partial y^3} = \exp(t) \cos(x - y), \quad (3)$$

with $(t, x, y) \in [0, T] \times \Omega$, $T > 0$, $\Omega = [0, 1.0] \times [0, 1.0]$, subject to the initial condition

$$u(0, x, y) = \sin(x - y) \quad (4)$$

and time-dependent boundary conditions

$$\left. \begin{aligned} u(t, x, 0) &= \exp(t) \cos(x), & u(t, x, 1) &= \exp(t) \cos(1 - x) \\ u(t, 0, y) &= \exp(t) \cos(y), & u(t, 1, y) &= \exp(t) \cos(1 - y) \end{aligned} \right\}. \quad (5)$$

The exact solution is

$$u(t; x, y) = \exp(t) \cos(x - y), \quad (6)$$

The paper is organized as follows. The two numerical experiments considered are described in Section 2. Section 3 describes the methodology of the reduced differential transform method (RDTM). In Section 4, we apply the RDTM to solve the homogeneous 1D and the 2D non-homogeneous dispersive KdV-type equations given in Equations (2) and (3), respectively. Section 5 is devoted to the application of the classical finite difference method to solve the considered numerical experiments in Section 2. This section also compares numerical results with the approximate series solutions obtained via RDTM. The obtained numerical results demonstrate the significant features such as efficiency and stability of the proposed schemes, and hence the employed techniques may be considered to solve other nonlinear as well as fractional problems. Section 6 highlights the salient features of the present study.

3. Reduced Differential Transform Method (RDTM)

Zhao [25] introduced differential transform method (DTM) to solve PDEs involved in electric circuit problems. DTM involves Taylor series expansion, which gives a polynomial series solution via an iterative procedure. Reduced differential transform method (RDTM) is very powerful method to obtain analytical approximate solutions to linear and nonlinear partial differential equations [18] and for systems of differential equations [12]. Basic definitions and properties for RDTM can be found in [7, 18, 19].

Definition 3.1 Consider a function of $n + 1$ variables. The reduced differential transform of $u(\tilde{X}, t) = u(x_1, x_2, \dots, x_n, t)$ (where $\tilde{X} \in \mathbb{R}^n$) with respect to t is defined by

$$U_k(\tilde{X}) = \frac{1}{k!} \left[\frac{\partial^k}{\partial t^k} u(\tilde{X}, t) \right]_{t=0}, \quad k = 0, 1, 2, \dots, \quad (7)$$

where $U_k(\tilde{X})$ denotes the transform function of $u(\tilde{X}, t)$.

Definition 3.2 The differential inverse transform of $\{U_k(\tilde{X})\}_{k=0}^n$ is defined by

$$u(\tilde{X}, t) = \sum_{k=0}^{\infty} U_k(\tilde{X}) t^k. \quad (8)$$

By substituting Equation (7) into Equation (8), we obtain

$$u(\tilde{X}, t) = \sum_{k=0}^{\infty} \frac{1}{k!} \left[\frac{\partial^k}{\partial t^k} u(\tilde{X}, t) \right]_{t=0} t^k.$$

From the above definitions, we see that RDTM is obtained from power series expansion. Please note that RDTM is close to the one dimensional DTM because RDTM is considered to be the standard DTM of $u(x, t)$ with respect to the variable t . However, the corresponding recursive algebraic equation is the function of the variable $\tilde{X} = (x_1, x_2, \dots, x_n)$.

The fundamental mathematical operations for RDTM [18, 19] are listed in Table 1.

Table 1: Transformed functions using RDTM

Function $f(\tilde{X}, t)$	Transformed function $F_k(\tilde{X})$
$au(\tilde{X}, t) \pm bv(\tilde{X}, t)$	$aU_k(\tilde{X}) \pm bV_k(\tilde{X})$
$u(\tilde{X}, t) \cdot v(\tilde{X}, t)$	$\sum_{i=0}^k U_i(\tilde{X}) \cdot V_{k-i}(\tilde{X})$
$\frac{\partial^n}{\partial t^n} u(\tilde{X}, t)$	$\frac{(k+n)!}{k!} U_{k+n}(\tilde{X})$
$\frac{\partial^n}{\partial x_i^n} u(\tilde{X}, t)$	$\frac{\partial^n U_k(\tilde{X})}{\partial x_i^n}$
$x^m t^n u(\tilde{X}, t)$	$\tilde{X}^{\tilde{m}} t^n U_{k-n}(\tilde{X})$ (where $\tilde{X}^{\tilde{m}} = x_1^{m_1} x_2^{m_2} \dots x_n^{m_n}$)
$\sin(\alpha x + \beta y + \gamma z + w t)$	$\frac{w^k}{k!} \cdot \sin\left(\frac{k\pi}{2!} + \alpha x + \beta y + \gamma z\right)$
$\cos(\alpha x + \beta y + \gamma z + w t)$	$\frac{w^k}{k!} \cdot \cos\left(\frac{k\pi}{2!} + \alpha x + \beta y + \gamma z\right)$
$\exp(\lambda t + \mu x)$	$\frac{\lambda^k}{k!} \cdot \exp(\mu x)$

To set forth the reduced differential transform approach, consider the operator form of the general PDE

$$\mathfrak{L}_t u(\tilde{X}, t) + \mathfrak{R}u(\tilde{X}, t) + \mathfrak{N}u(\tilde{X}, t) = g(\tilde{X}, t), \quad (9)$$

with initial condition $u(\tilde{X}, 0) = h(\tilde{X})$, where $\mathfrak{L}_t = \frac{\partial}{\partial t}$, \mathfrak{R} is a linear operator that includes partial derivatives with respect to \tilde{X} , \mathfrak{N} is a nonlinear operator and g is a non-homogeneous term, which is u -independent.

According to the procedures of RDTM and Table 1, we can construct the following recursive formula:

$$(k+1) U_{k+1}(\tilde{X}) = G_k(\tilde{X}) - \mathfrak{R}U_k(\tilde{X}) - \mathfrak{N}U_k(\tilde{X}), \quad (10)$$

where $U_k(\tilde{X})$, $\mathfrak{R}U_k(\tilde{X})$, $\mathfrak{N}U_k(\tilde{X})$ and $G_k(\tilde{X})$ are the transformations of the functions $\mathfrak{L}_t u(\tilde{X}, t)$, $\mathfrak{R}u(\tilde{X}, t)$, $\mathfrak{N}u(\tilde{X}, t)$ and $g(\tilde{X}, t)$. From initial condition $u(\tilde{X}, 0) = f(\tilde{X})$, we write

$$U_0(\tilde{X}) = f(\tilde{X}). \quad (11)$$

Substituting Equation (11) into Equation (10) and using a straightforward iterative computation, we obtain the values of $U_k(\tilde{X})$ for $k = 1, 2, \dots, n$. Then, the inverse transformation of $\{U_k(\tilde{X})\}_{k=0}^n$ gives the approximation solution as

$$\bar{u}_n(\tilde{X}, t) = \sum_{k=0}^n U_k(\tilde{X}) t^k, \quad (12)$$

where n is the order of approximation solution. Therefore, the exact solution is given by

$$u(\tilde{X}, t) = \lim_{n \rightarrow \infty} \bar{u}_n(\tilde{X}, t). \quad (13)$$

3.1. Application of RDTM to the 1D-dispersive Nonlinear KdV Equation

Consider the homogeneous nonlinear KdV equation

$$u_t + 6uu_x + u_{xxx} = 0, \quad (14)$$

with initial condition

$$u(x, 0) = x. \quad (15)$$

By now applying differential transform of Equation (14) and the initial condition (15), respectively,

$$(k+1) U_{k+1}(x) + 6 \sum_{r=0}^k U_r(x) \frac{\partial U_{k-r}(x)}{\partial x} + \frac{\partial^3 U_k(x)}{\partial x^3} = 0, \quad (16)$$

where the t -dimensional spectrum function $U_k(x)$ are the transformed functions.

From the initial condition (15), we write

$$U_0(x) = x. \quad (17)$$

By now substituting Equation (17) into Equation (16), we obtain the following $U_k(x)$ values successively:

$$U_1(x) = -6U_0(x) \frac{\partial U_0(x)}{\partial x} - \frac{\partial^3 U_0(x)}{\partial x^3} = -6x,$$

$$U_2(x) = -\frac{6}{2} \cdot \left(U_0(x) \frac{\partial U_1(x)}{\partial x} + U_1(x) \frac{\partial U_0(x)}{\partial x} \right) - \frac{1}{2} \frac{\partial^3 U_1(x)}{\partial x^3} = 36x = 6^2 x,$$

$$U_3(x) = -\frac{6}{3} \cdot \left(U_0(x) \frac{\partial U_2(x)}{\partial x} + U_1(x) \frac{\partial U_1(x)}{\partial x} + U_2(x) \frac{\partial U_0(x)}{\partial x} \right) - \frac{1}{3} \frac{\partial^3 U_2(x)}{\partial x^3} = -216x = -6^3 x,$$

$$U_4(x) = -\frac{6}{4} \cdot \left(U_0(x) \frac{\partial U_3(x)}{\partial x} + U_1(x) \frac{\partial U_2(x)}{\partial x} + U_2(x) \frac{\partial U_1(x)}{\partial x} + U_3(x) \frac{\partial U_0(x)}{\partial x} \right) - \frac{1}{4} \frac{\partial^3 U_3(x)}{\partial x^3} = 1296x = 6^4 x,$$

$$U_5(x) = -\frac{6}{5} \cdot \left(U_0(x) \frac{\partial U_4(x)}{\partial x} + U_1(x) \frac{\partial U_3(x)}{\partial x} + U_2(x) \frac{\partial U_2(x)}{\partial x} + U_3(x) \frac{\partial U_1(x)}{\partial x} + U_4(x) \frac{\partial U_0(x)}{\partial x} \right) - \frac{1}{5} \frac{\partial^3 U_4(x)}{\partial x^3} = -7776x = -6^5 x$$

and so on. Then, by applying the differential-inverse transform $\{U_k(x)\}_{k \geq 0}$ gives the following approximate solution

$$\begin{aligned} u(x, t) &= \sum_{k \geq 0} U_k(x) t^k = x - 6xt + 36xt^2 - 216xt^3 + 1296xt^4 - 7776xt^5 + \dots \\ &= x [1 - 6t + (6t)^2 - (6t)^3 + (6t)^4 - (6t)^5 + \dots] = \frac{x}{1+6t}, \quad \text{for } |-6t| < 1, \end{aligned} \quad (18)$$

which coincides with the exact solution of Equation (2).

Plots of exact and numerical solution vs x are displayed in Figure 1. We obtain plots of absolute error vs x at three different values of time in Figure 2.

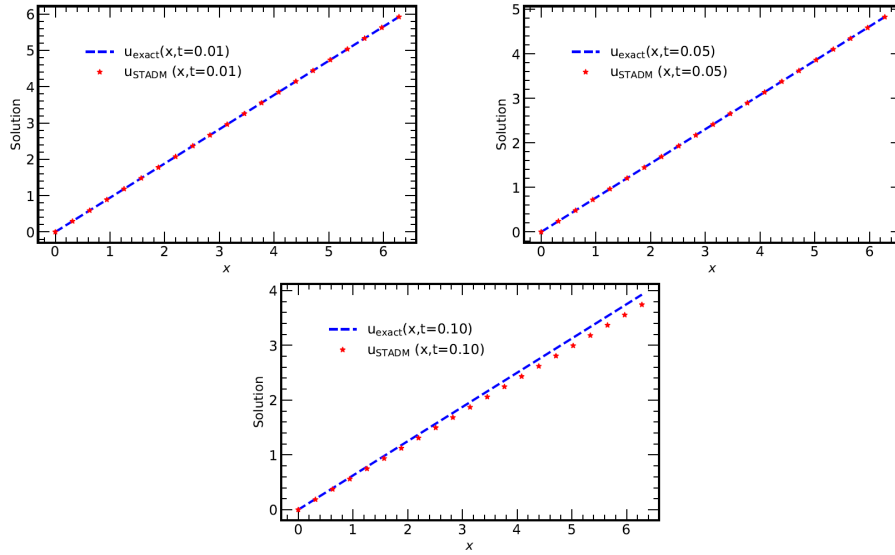


Figure 1: Plots of exact solution and approximate solution using RDTM (5-terms) vs x at times 0.01, 0.05, 0.10 (The space interval used for these plots is $\frac{\pi}{10} \approx 0.314$)

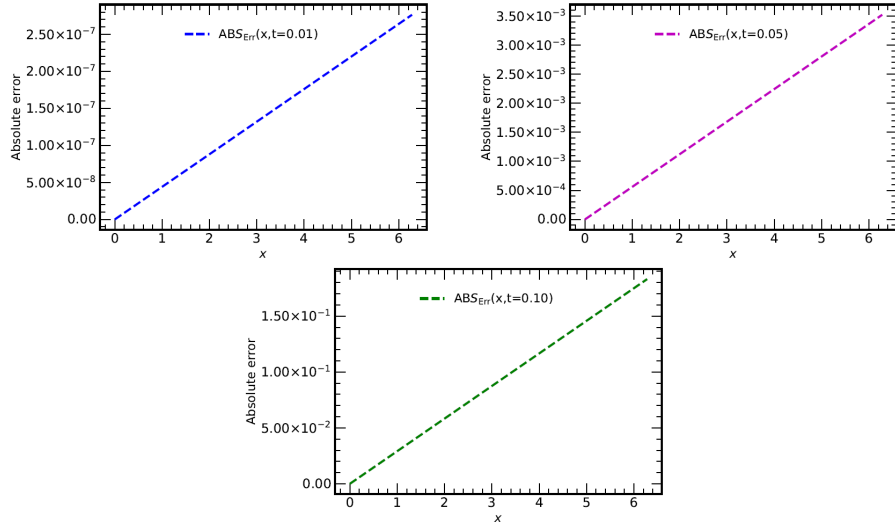


Figure 2: Plots of absolute errors vs x at times ($t = 0.01, 0.05, 0.10$), using RDTM (5-terms)

The absolute error and relative errors at a given spatial node x_j and given time t_n are obtained as follows:

$$\text{Absolute Error} = |u(x_j, t_n) - U(x_j, t_n)|,$$

$$\text{Relative Error} = \frac{|u(x_j, t_n) - U(x_j, t_n)|}{|u(x_j, t_n)|},$$

where $u(x_j, t_n)$ denotes the exact solution and $U(x_j, t_n)$ is the numerical solution at a given spatial node x_j and given time t_n .

We also compare the absolute and relative errors at some values of x at three different times in Table 2.

Table 2: Absolute and Relative errors at times ($t = 0.01, 0.05, 0.1$), using RDTM

t	Values of x	Exact solution	Numerical solution	Absolute error	Relative error
0.01	0.000	0.000000	0.000000	0.000000	—
	0.314	0.296226	0.296226	1.382074×10^{-8}	4.665600×10^{-8}
	0.942	0.888679	0.888679	4.146222×10^{-8}	4.665600×10^{-8}
	1.570	1.481132	1.481132	6.910370×10^{-8}	4.665600×10^{-8}
	2.198	2.073585	2.073585	9.674518×10^{-8}	4.665600×10^{-8}
	2.826	2.666038	2.666038	1.243867×10^{-7}	4.665600×10^{-8}
	3.454	3.258491	3.258490	1.520281×10^{-7}	4.665600×10^{-8}
	4.082	3.850943	3.850943	1.796696×10^{-7}	4.665600×10^{-8}
	4.710	4.443396	4.443396	2.073111×10^{-7}	4.665600×10^{-8}
	5.338	5.035849	5.035849	2.349526×10^{-7}	4.665600×10^{-8}
0.05	0.000	0.000000	0.000000	0.000000	—
	0.314	0.241538	0.241362	1.760815×10^{-4}	7.290000×10^{-4}
	0.942	0.724615	0.724087	5.282446×10^{-4}	7.290000×10^{-4}
	1.570	1.207692	1.206812	8.804077×10^{-4}	7.290000×10^{-4}
	2.198	1.690769	1.689537	1.232571×10^{-3}	7.290000×10^{-4}
	2.826	2.173846	2.172261	1.584734×10^{-3}	7.290000×10^{-4}
	3.454	2.656923	2.654986	1.936897×10^{-3}	7.290000×10^{-4}
	4.082	3.140000	3.137711	2.289060×10^{-3}	7.290000×10^{-4}
	4.710	3.623077	3.620436	2.641223×10^{-3}	7.290000×10^{-4}
	5.338	4.106154	4.103160	2.993386×10^{-3}	7.290000×10^{-4}
0.10	0.000	0.000000	0.000000	0.000000	—
	0.314	0.196250	0.187094	9.156240×10^{-3}	4.665600×10^{-2}
	0.942	0.588750	0.561281	2.746872×10^{-2}	4.665600×10^{-2}
	1.570	0.981250	0.935469	4.578120×10^{-2}	4.665600×10^{-2}
	2.198	1.373750	1.309656	6.409368×10^{-2}	4.665600×10^{-2}
	2.826	1.766250	1.683844	8.240616×10^{-2}	4.665600×10^{-2}
	3.454	2.158750	2.058031	1.007186×10^{-1}	4.665600×10^{-2}
	4.082	2.551250	2.432219	1.190311×10^{-1}	4.665600×10^{-2}
	4.710	2.943750	2.806406	1.373436×10^{-1}	4.665600×10^{-2}
	5.338	3.336250	3.180594	1.556561×10^{-1}	4.665600×10^{-2}
5.966	3.728750	3.554781	1.739686×10^{-1}	4.665600×10^{-2}	
6.280	3.925000	3.741875	1.831248×10^{-1}	4.665600×10^{-2}	

Remark 3.3 Table 2 shows that RDTM is very effective at small and medium propagation time but become less effective at longer propagation time. Some real life applications where solving KdV equation over short propagation involve weather forecast after Tsunami, Tectonic scenarios and earth quake modeling and simulation of optical laser short pulses along fibres.

4. Application of RDTM to the 2D-Linearized KdV Equation

We now show the applicability of RDTM to solve Equation (3). If we apply RDTM to Equations (3) and (4) and using Table 1, we obtain the following recursive equation

$$U_{k+1}(x, y) = -\frac{1}{k+1} \left\{ \frac{\partial^3 U_k(x, y)}{\partial x^3} + \frac{\partial^3 U_k(x, y)}{\partial y^3} - \cos(x-y) \left(\frac{1}{k!} \right) \right\}. \quad (19)$$

From Equation (7), the initial conditions given in Equation (4) can be transformed at $t = 0$ as

$$U_0(x, y) = \cos(x-y). \quad (20)$$

Substituting the transformed condition of Equation (20) into Equation (19) and by a straightforward iterative steps, the following $U_k(t, x, y)$, $k = 0, 1, 2, \dots, n$ values are obtained:

$$\left. \begin{aligned}
 U_1(x, y) &= -(-U_{0,3x} + U_{0,3y}) + \cos(x - y) = \cos(x - y) \\
 U_2(x, y) &= -\frac{1}{2} \cdot (-U_{1,3x} + U_{1,3y}) + \cos(x - y) = \frac{1}{2!} \cos(x - y) \\
 U_3(x, y) &= -\frac{1}{3} \cdot (-U_{2,3x} + U_{2,3y}) + \frac{1}{2!} \cos(x - y) = \frac{1}{3!} \cos(x - y) \\
 U_4(x, y) &= -\frac{1}{4} \cdot (-U_{3,3x} + U_{3,3y}) + \frac{1}{3!} \cos(x - y) = \frac{1}{4!} \cos(x - y) \\
 U_5(x, y) &= -\frac{1}{5} \cdot (-U_{4,3x} + U_{4,3y}) + \frac{1}{4!} \cos(x - y) = \frac{1}{5!} \cos(x - y) \\
 U_6(x, y) &= -\frac{1}{6} \cdot (-U_{5,3x} + U_{5,3y}) + \frac{1}{5!} \cos(x - y) = \frac{1}{6!} \cos(x - y) \\
 U_7(x, y) &= -\frac{1}{7} \cdot (-U_{6,3x} + U_{6,3y}) + \frac{1}{6!} \cos(x - y) = \frac{1}{7!} \cos(x - y) \\
 U_8(x, y) &= -\frac{1}{8} \cdot (-U_{7,3x} + U_{7,3y}) + \frac{1}{7!} \cos(x - y) = \frac{1}{8!} \cos(x - y) \\
 U_9(x, y) &= -\frac{1}{9} \cdot (-U_{8,3x} + U_{8,3y}) + \frac{1}{8!} \cos(x - y) = \frac{1}{9!} \cos(x - y) \\
 U_{10}(x, y) &= -\frac{1}{10} \cdot (-U_{9,3x} + U_{9,3y}) + \frac{1}{9!} \cos(x - y) = \frac{1}{(10)!} \cos(x - y)
 \end{aligned} \right\}, \quad (21)$$

where $U_{k,x}(x, y) = \frac{\partial U^k(x, y)}{\partial x^k}$. We can easily inspect from Equation (21) that the concise formulation, after many iterations, takes the form

$$U_k(x, y) = \frac{(-1)^{2k}}{(k)!} \cdot \cos(x - y), \quad \text{for } k \in \mathbb{Z}^+.$$

Then, using the inverse transformation in Equation (8) of the set of values of $\{U_k(x, y)\}_{k=0}^n$ gives the tenth-order approximate solution as

$$u(t, x, y) \approx \sum_{k=0}^{10} U_k(x, y) t^k = \cos(x - y) \left\{ 1 + t + \frac{t^2}{2!} + \frac{t^3}{3!} + \frac{t^4}{4!} + \frac{t^5}{5!} + \frac{t^6}{6!} + \frac{t^7}{7!} + \frac{t^8}{8!} + \frac{t^9}{9!} + \frac{t^{10}}{(10)!} + \dots \right\},$$

which coincides with the exact solution given in Equation (6) on the limit.

As an illustration of the application of RDTM, Tables 3-5 shows absolute and relative errors for the 2D linearized dispersive KdV equation given in Equation (3) using the first ten-terms of the approximate solution by RDTM. Graphical representation of the exact and RDTM solution is shown in Figures 3 - 5.

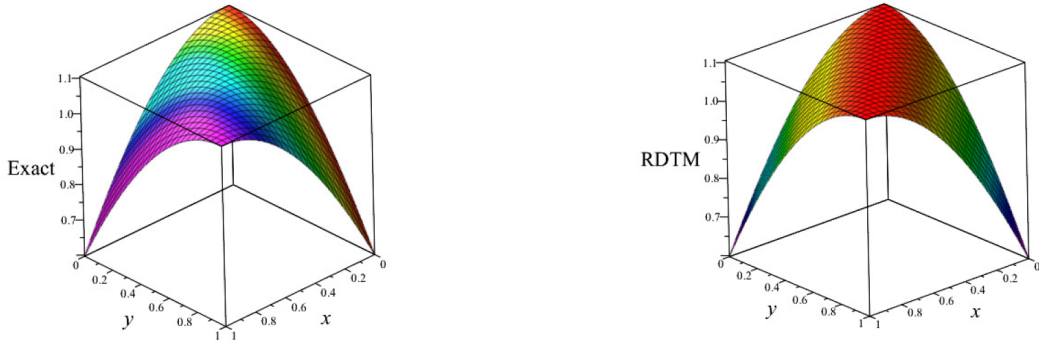


Figure 3: Graphs of the exact and numerical solution via RDTM for Equation (3) on $\Omega = (0, 1)^2$ at $t = 0.10$ used spatial step sizes $\Delta x = \Delta y = 0.1$

Table 3: A comparison between the exact solution and RDTM solution at some values of x and y at time $t = 0.10$

t	x	y	Exact	RDTM	Absolute error	Relative error
0.0	0.0	0.0	1.105171	1.105171	4.440892×10^{-16}	4.018285×10^{-16}
		0.2	1.105171	1.105171	4.440892×10^{-16}	4.018285×10^{-16}
		0.4	1.083141	1.083141	4.440892×10^{-16}	4.100013×10^{-16}
		0.6	1.017929	1.017929	4.440892×10^{-16}	4.362670×10^{-16}
		0.8	9.121369×10^{-1}	9.121369×10^{-1}	3.330669×10^{-16}	3.651501×10^{-16}
0.10	0.4	0.2	1.083141	1.083141	4.440892×10^{-16}	4.100013×10^{-16}
		0.4	1.105171	1.105171	4.440892×10^{-16}	4.018285×10^{-16}
		0.6	1.083141	1.083141	4.440892×10^{-16}	4.100013×10^{-16}
		0.8	1.017929	1.017929	4.440892×10^{-16}	4.362670×10^{-16}
0.6	0.2	0.2	1.017929	1.017929	4.440892×10^{-16}	4.362670×10^{-16}
		0.4	1.083141	1.083141	4.440892×10^{-16}	4.100013×10^{-16}
		0.6	1.105171	1.105171	4.440892×10^{-16}	4.018285×10^{-16}
		0.8	1.083141	1.083141	4.440892×10^{-16}	4.100013×10^{-16}
0.8	0.2	9.121369×10^{-1}	9.121369×10^{-1}	3.330669×10^{-16}	3.651501×10^{-16}	
		0.4	1.017929	1.017929	4.440892×10^{-16}	4.362670×10^{-16}
		0.6	1.083141	1.083141	4.440892×10^{-16}	4.100013×10^{-16}
		0.8	1.105171	1.105171	4.440892×10^{-16}	4.018285×10^{-16}
1.0	1.0	1.105171	1.105171	4.440892×10^{-16}	4.018285×10^{-16}	

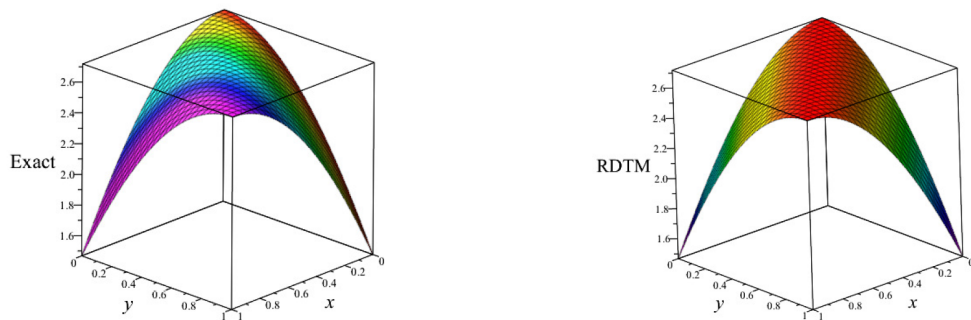


Figure 4: Graphs of the exact and numerical solution via RDTM of Equation. (3) on $\Omega = (0, 1)^2$ at $t = 1.0$ used spatial step sizes $\Delta x = \Delta y = 0.1$

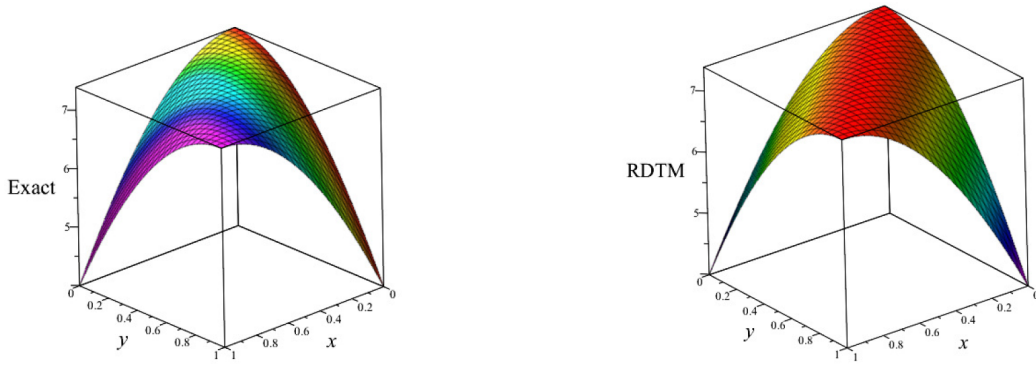


Figure 5: Graphs of the exact and numerical solution via RDTM of Equation (3) on $\Omega = (0, 1)^2$ at $t = 2.0$ used spatial step sizes $\Delta x = \Delta y = 0.1$

Table 4: A comparison between the exact solution and RDTM solution at some values of x and y at time $t = 1.0$

t	x	y	Exact	RDTM	Absolute error	Relative error
0.0	0.0	0.0	2.718282	2.718282	2.731266×10^{-8}	1.004777×10^{-8}
		0.2	2.718282	2.718282	2.731266×10^{-8}	1.0047766×10^{-8}
		0.4	2.664097	2.664097	2.676823×10^{-8}	1.004777×10^{-8}
		0.6	2.503703	2.503703	2.515663×10^{-8}	1.004777×10^{-8}
1.0	0.4	0.2	2.664097	2.664097	2.676823×10^{-8}	1.004777×10^{-8}
		0.4	2.718282	2.718282	2.731266×10^{-8}	1.004777×10^{-8}
		0.6	2.664097	2.664097	2.676823×10^{-8}	1.004777×10^{-8}
		0.8	2.503703	2.503703	2.515663×10^{-8}	1.004777×10^{-8}
0.6	0.2	0.2	2.503703	2.503703	2.515663×10^{-8}	1.004777×10^{-8}
		0.4	2.664097	2.664097	2.676823×10^{-8}	1.004777×10^{-8}
		0.6	2.718282	2.718282	2.731266×10^{-8}	1.004777×10^{-8}
		0.8	2.664097	2.664097	2.676823×10^{-8}	1.004777×10^{-8}
0.8	0.2	0.2	2.243495	2.243495	2.254211×10^{-8}	1.004777×10^{-8}
		0.4	2.503703	2.503703	2.515663×10^{-8}	1.004777×10^{-8}
		0.6	2.664097	2.664097	2.6768226×10^{-8}	1.004777×10^{-8}
		0.8	2.718282	2.718282	2.731266×10^{-8}	1.004777×10^{-8}
1.0	1.0	2.718282	2.718282	2.731266×10^{-8}	1.0047766×10^{-8}	

Table 5: A comparison between the exact solution and RDTM solution at some values of x and y at time $t = 2.0$

t	x	y	Exact	RDTM	Absolute error	Relative error
0.0	0.0	0.0	7.389056	7.388995	6.138994×10^{-5}	8.308224×10^{-6}
		0.2	7.389056	7.38899	6.138994×10^{-5}	8.308224×10^{-6}
		0.4	7.241767	7.241707	6.016622×10^{-5}	8.308224×10^{-6}
		0.6	6.805771	6.805715	5.654388×10^{-5}	8.308224×10^{-6}
		0.8	6.098451	6.098400	5.066730×10^{-5}	8.308224×10^{-6}
2.0	0.4	0.2	7.241767	7.241707	6.016622×10^{-5}	8.308224×10^{-6}
		0.4	7.389056	7.388995	6.138994×10^{-5}	$8.30822437 \times 10^{-6}$
		0.6	7.241767	7.241707	6.016622×10^{-5}	8.308224×10^{-6}
		0.8	6.8057714	6.805715	5.654388×10^{-5}	8.308224×10^{-6}
0.6	0.2	0.2	6.805771	6.805715	5.654388×10^{-5}	8.308224×10^{-6}
		0.4	7.241767	7.241707	6.016622×10^{-5}	8.308224×10^{-6}
		0.6	7.389056	7.388995	6.138994×10^{-5}	8.308224×10^{-6}
		0.8	7.241767	7.241707	6.016622×10^{-5}	8.308224×10^{-6}
0.8	0.2	0.2	6.098451	6.098400	5.066730×10^{-5}	8.308224×10^{-6}
		0.4	6.805771	6.805715	5.654388×10^{-5}	8.308224×10^{-6}
		0.6	7.241767	7.241707	6.016622×10^{-5}	8.308224×10^{-6}
		0.8	7.389056	7.388995	6.138994×10^{-5}	8.308224×10^{-6}
1.0	1.0	7.389056	7.388995	6.138994×10^{-5}	8.308224×10^{-6}	

Remark 4.1 Tables 3 - 5 provide comparison between exact and RDTM solution with corresponding absolute and relative errors given. The relative error is of order 10^{-16} at $t = 0.10$, of order 10^{-8} at time $t = 1.0$ and of order 10^{-6} at $t = 2.0$.

5. Classical Finite Difference Method

In this section, we employ the classical finite difference method to solve some dispersive KdV equations and we also compare the numerical results with the RDTM method. The following central-difference approximations can be used to handle derivatives used in the numerical experiments:

$$\left. \begin{aligned} \frac{\partial u}{\partial t} \Big|_i^n &\approx \frac{u_i^{n+1} - u_i^{n-1}}{2\Delta t} \\ \frac{\partial u}{\partial x} \Big|_i^n &\approx \frac{u_{i+1}^n - u_{i-1}^n}{2\Delta x} \\ \frac{\partial^3 u}{\partial x^3} \Big|_i^n &\approx \frac{u_{i+2}^n - 2u_{i+1}^n + 2u_{i-1}^n - u_{i-2}^n}{2(\Delta x)^3} \end{aligned} \right\}, \quad (22)$$

where $h = \Delta x$ and $k = \Delta t$ are the spatial and temporal step sizes, respectively and $x_i = (i-1) \cdot h$, $t_j = (j-1) \cdot k$, $i = 1, 2, \dots$ and $j = 1, 2, \dots$, where superscript j denotes a quantity associated with time level t_j and subscript i denotes a quantity associated with space mesh point x_i .

5.1. Solution of Numerical Experiment 1 Using Finite Difference Scheme

Let's consider the homogeneous dispersive KdV equation

$$\left. \begin{aligned} u_t + 6uu_x + u_{xxx} &= 0 \\ u(x, 0) &= 0 \end{aligned} \right\}. \quad (23)$$

By using the method proposed by Zabusky-Kruskal in [24], Equation (23) is discretized as

$$\frac{u_i^{n+1} - u_i^{n-1}}{2\Delta t} = -6 \left(\frac{u_{i-1}^n + u_i^n + u_{i+1}^n}{3} \right) \left(\frac{u_{i+1}^n - u_{i-1}^n}{2\Delta x} \right) - \left(\frac{u_{i+2}^n - 2u_{i+1}^n + 2u_{i-1}^n - u_{i-2}^n}{2(\Delta x)^3} \right). \quad (24)$$

The scheme is given by

$$u_i^{n+1} = u_i^{n-1} - \frac{2\Delta t}{\Delta x} \cdot (u_{i-1}^n + u_i^n + u_{i+1}^n) (u_{i+1}^n - u_{i-1}^n) - \frac{\Delta t}{(\Delta x)^3} \cdot (u_{i+2}^n - 2u_{i+1}^n + 2u_{i-1}^n - u_{i-2}^n). \quad (25)$$

We next study the stability of the scheme. Using Von Neumann stability analysis [9] and freezing coefficient technique [21], we get

$$\xi^2 + \mathcal{S}\xi - 1 = 0, \quad (26)$$

where

$$\left. \begin{aligned} \mathcal{S} &= (12u_{\max}\lambda I \sin(\omega)) + \frac{\lambda}{h^2} (2I \sin(2\omega) - 4I \sin(\omega)) \\ \lambda &= \frac{k}{h}, \quad I = \sqrt{-1} \end{aligned} \right\}. \quad (27)$$

Solving Equation (26) gives

$$\xi = \frac{-\mathcal{S} \pm \sqrt{\mathcal{S}^2 + 4}}{2}, \quad (28)$$

where \mathcal{S} is given in Equation (27). A condition for stability criterion is obtained by finding a condition for $\Delta t, \Delta x$ so that for all θ, ξ an inequality $|\xi| \leq 1$ is true; that is,

$$4 - \left(12u_{\max}\lambda \sin(\omega) + \frac{\lambda}{h^2} (2 \sin(2\omega) - 4 \sin(\omega)) \right)^2 \geq 0, \quad (29)$$

which gives $|\{12u_{\max}\lambda \sin(2\omega) + \frac{\lambda}{h^2} (2 \sin(2\omega) - 4 \sin(\omega))\}| \leq 2$.

Since the second expression in the bracket for the above inequality dominates the first for small values of h , we obtain $\omega = \frac{2\pi}{3}$ from the second expression which gives the maximum value for the inequality.

On substituting this into the inequality, we obtain the region of stability as

$$|\lambda| \leq \frac{2}{|\{12u_{\max} \sin(2\omega) + \frac{1}{h^2} (2 \sin(2\omega) - 4 \sin(\omega))\}|} \leq \left| \frac{2}{6\sqrt{3}u_{\max} - \frac{3\sqrt{3}}{h^2}} \right| = \left| \frac{2}{3\sqrt{3}(2u_{\max} - \frac{1}{h^2})} \right|. \quad (30)$$

By considering $h = \Delta x = \frac{\pi}{10}$ and using Equation (30), we obtain

$$0 < \Delta t \leq \frac{0.3849002}{2u_{max} - 10.142399}. \quad (31)$$

By choosing $u_{max} = 2\pi \approx 6.283$, Equation (31) gives $0 < \Delta t \leq 9.973539 \times 10^{-2}$. We run the experiment with $\Delta x = \frac{\pi}{10} \approx 0.314$ and $\Delta t = 0.0001$.

We obtain plots of numerical and exact profiles vs x in Figure 6 and corresponding plots of absolute errors vs x are shown in Figure 7.

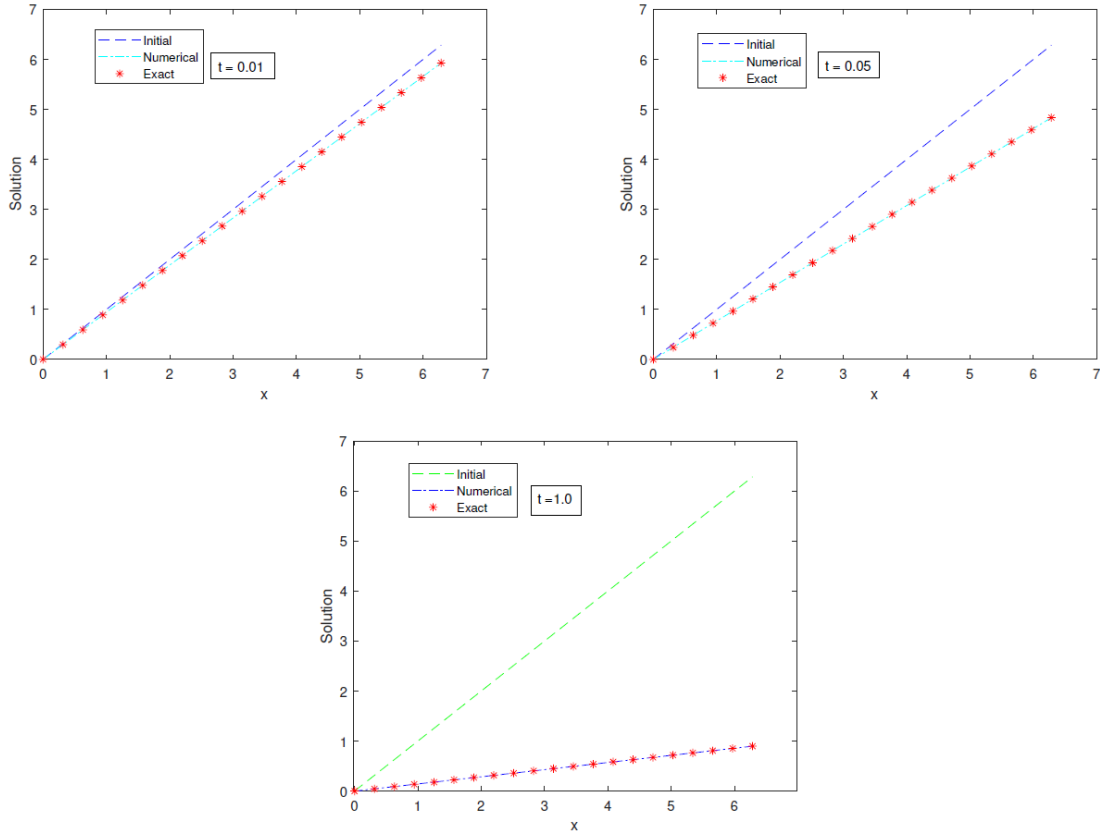


Figure 6: Plots of exact solution and approximate solution at times 0.01, 0.05, 1.0, using classical finite difference scheme with $k = 0.0001$ and $h = \frac{\pi}{10} = 0.314$

Table 6: Absolute/Relative errors at times ($t = 0.01, 0.05, 1.0$), using classical finite difference scheme with $k = 0.0001$ (Numerical experiment 1)

t	Values of x	Exact solution	Numerical solution	Absolute error	Relative error
0.01	0.000	0.0000000	0.0000000	0.000000	—
	0.314	0.1963495	0.1963495	0.000000	0.000000
	0.942	0.5890486	0.5890489	3.1041015×10^{-7}	5.2696863×10^{-7}
	1.570	0.98174770	0.9817485	7.8652172×10^{-7}	8.0114444×10^{-7}
	2.198	1.3744468	1.3744478	9.6077894×10^{-7}	6.9902953×10^{-7}
	2.826	1.7671459	1.7671470	1.1365772×10^{-6}	6.4317115×10^{-7}
	3.454	2.1598449	2.1598462	1.2485592×10^{-6}	5.7807814×10^{-7}
	4.082	2.5525440	2.5525456	6.3715406×10^{-7}	2.496153×10^{-7}
	4.710	2.9452431	2.9452430	$7.43802406 \times 10^{-8}$	2.5254364×10^{-8}
	5.338	3.3379422	3.3379419	3.1556491×10^{-7}	9.4538759×10^{-8}
	5.966	3.7306413	3.7306413	0.000000	0.000000
6.280	5.9275333	5.9275333	0.000000	0.000000	
0.05	0.000	0.0000000	0.0000000	0.000000	—
	0.314	0.24166097	0.24166097	0.0000000	0.000000
	0.942	0.72498292	0.72498312	2.3812425×10^{-7}	3.2845498×10^{-7}
	1.570	1.2083049	1.2083053	4.2702059×10^{-7}	3.5340467×10^{-7}
	2.198	1.6916268	1.6916274	5.4596386×10^{-7}	3.2274486×10^{-7}
	2.826	2.17494876	2.1749495	6.9540557×10^{-7}	3.1973423×10^{-7}
	3.454	2.6582707	2.6582715	8.2595631×10^{-7}	3.1071189×10^{-7}
	4.082	3.1415927	3.1415935	8.3089143×10^{-7}	2.6448096×10^{-7}
	4.710	3.6249146	3.6249151	4.9807088×10^{-7}	1.3740210×10^{-7}
	5.338	4.1082365	4.1082364	1.6124848×10^{-7}	3.925005×10^{-8}
	5.966	4.5915585	4.5915585	0.0000000	0.0000000
6.280	4.8332195	4.8332195	0.0000000	0.0000000	
1.0	0.000	0.0000000	0.0000000	0.0000000	—
	0.314	0.0448799	0.0448799	0.0000000	0.0000000
	0.942	0.1346397	0.1346395	1.4962311×10^{-7}	1.1112852×10^{-6}
	1.570	0.2243995	0.2243997	2.3736019×10^{-7}	1.0577573×10^{-6}
	2.198	0.3141593	0.3141606	1.3373548×10^{-6}	4.2569325×10^{-6}
	2.826	0.4039191	0.4039205	1.4249419×10^{-6}	3.5277909×10^{-6}
	3.454	0.4936788	0.4936786	2.8213009×10^{-7}	5.7148508×10^{-7}
	4.082	0.5834386	0.5834377	9.8115697×10^{-7}	1.6816798×10^{-6}
	4.710	0.6731984	0.6731999	1.4624647×10^{-6}	2.1724125×10^{-6}
	5.338	0.7629582	0.7629605	2.3306310×10^{-6}	3.0547295×10^{-8}
	5.966	0.8527180	0.8527180	0.00000000	0.00000000
6.280	0.8975979	0.8975974	0.00000000	0.00000000	

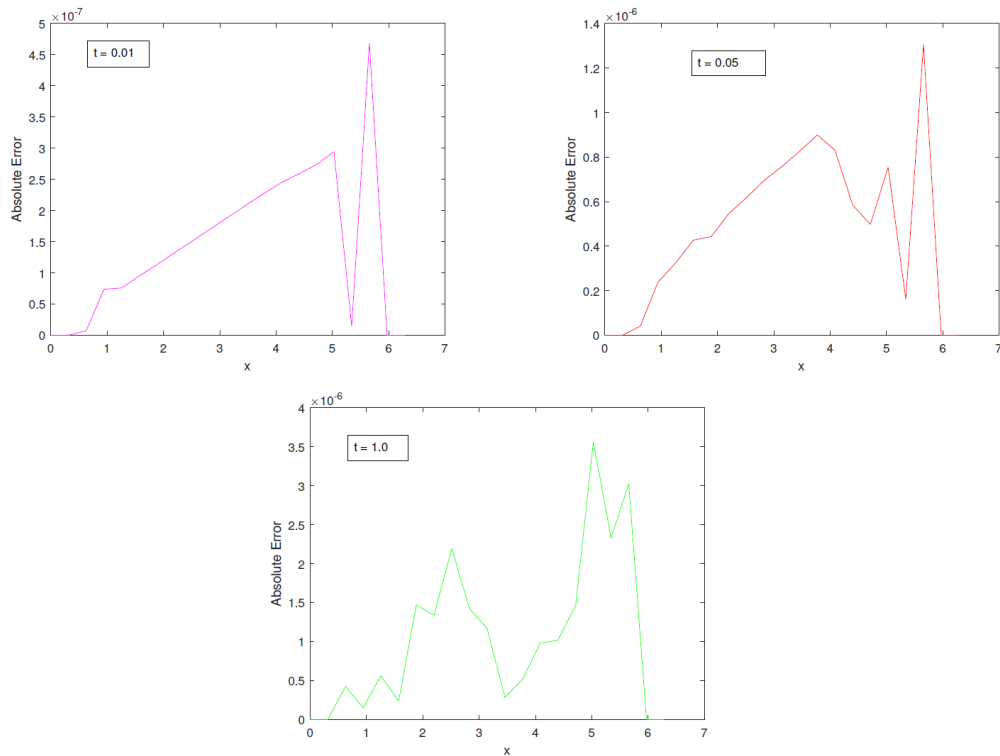


Figure 7: Plots of absolute errors vs x at different values of times $t = 0.01, 0.05, 1.0$, using classical finite difference scheme with $k = 0.0001$ and $h = \frac{\pi}{10}$

Remark 5.1 As shown in Figure 7, the scheme is very efficient at short, medium and long time propagation. Table 6 displays absolute and relative errors at the spatial nodes for the three different values of time, which indicates that the scheme is very efficient at short, medium and long time propagation.

5.2. Solution of Numerical Experiment 2 Using Classical FDM

This section employs a classical finite-difference method to solve Equation (3). We will also compare results with the approximate series solutions obtained via RDTM. In order to handle this, let's recall the following central difference approximations [11]:

$$\left. \begin{aligned} \frac{\partial u}{\partial t} \Big|_{i,j}^n &\approx \frac{U_{i,j}^{n+1} - U_{i,j}^{n-1}}{2 \cdot \Delta t} \\ \frac{\partial u}{\partial x} \Big|_{i,j}^n &\approx \frac{U_{i+1,j}^n - U_{i-1,j}^n}{2 \cdot \Delta x} \\ \frac{\partial^3 u}{\partial x^3} \Big|_{i,j}^n &\approx \frac{U_{i+2,j}^n - 2U_{i+1,j}^n + 2U_{i-1,j}^n - U_{i-2,j}^n}{2 \cdot (\Delta x)^3} \\ \frac{\partial^3 u}{\partial y^3} \Big|_{i,j}^n &\approx \frac{U_{i,j+2}^n - 2U_{i,j+1}^n + 2U_{i,j-1}^n - U_{i,j-2}^n}{2 \cdot (\Delta y)^3} \end{aligned} \right\}. \quad (32)$$

We point out that a rectangular domain is divided into square grids with each x and y -intervals of length Δx and Δy , respectively, whereas each t -interval is of length Δt . Without loss of generality, we consider uniform grid $\Delta x = \Delta y = h$, where

$$x_i = (i - 1) \cdot \Delta x = (i - 1) \cdot h, \quad i = 1, \dots, NP,$$

$$y_j = (j - 1) \cdot \Delta y = (j - 1) \cdot h, \quad j = 1, \dots, NP,$$

$$t_n = (n - 1) \cdot \Delta t = (n - 1) \cdot k, \quad n \in \mathbb{N}.$$

The discretized form of the scheme for Equation (3) is given by

$$\begin{aligned} \frac{U_{i,j}^{n+1} - U_{i,j}^{n-1}}{2\Delta t} &= - \left(\frac{U_{i+2,j}^n - 2U_{i+1,j}^n + 2U_{i-1,j}^n - U_{i-2,j}^n}{2 \cdot (\Delta x)^3} \right) - \left(\frac{U_{i,j+2}^n - 2U_{i,j+1}^n + 2U_{i,j-1}^n - U_{i,j-2}^n}{2 \cdot (\Delta y)^3} \right) \\ &+ \exp((K - 1) \times \Delta t) \cos((i - 1)\Delta x - (j - 1)\Delta y). \end{aligned} \quad (33)$$

Hence, the numerical scheme takes the form

$$\begin{aligned} U_{i,j}^{n+1} &= U_{i,j}^{n-1} - r_x (U_{i+2,j}^n - 2U_{i+1,j}^n + 2U_{i-1,j}^n - U_{i-2,j}^n) - r_y (U_{i,j+2}^n - 2U_{i,j+1}^n + 2U_{i,j-1}^n - U_{i,j-2}^n) \\ &+ \exp((K - 1) \times \Delta t) \cos((i - 1)\Delta x - (j - 1)\Delta y), \end{aligned} \quad (34)$$

where

$$r_x = \frac{\Delta t}{(\Delta x)^3} \quad \text{and} \quad r_y = \frac{\Delta t}{(\Delta y)^3}. \quad (35)$$

For stability, we use Von Neumann stability analysis as given in [9] by considering Equation (34) with source term to be zero since it is u -independent; i.e.,

$$U_{i,j}^{n+1} = U_{i,j}^{n-1} - r_x (U_{i+2,j}^n - 2U_{i+1,j}^n + 2U_{i-1,j}^n - U_{i-2,j}^n) - r_y (U_{i,j+2}^n - 2U_{i,j+1}^n + 2U_{i,j-1}^n - U_{i,j-2}^n). \quad (36)$$

Substituting $U_{i,j}^n$ by $\xi^n \cdot e^{I\omega_x i} \cdot e^{I\omega_y j}$ yields

$$\begin{aligned} \xi^{n+1} \exp [I(\omega_x i + \omega_y j)] &= \xi^{n-1} \exp [I(\omega_x i + \omega_y j)] - \frac{\Delta t}{(\Delta x)^3} \left(\xi^n \exp [I(\omega_x (i+2) + \omega_y j)] - 2\xi^n \exp [I(\omega_x (i+1) + \omega_y j)] \right. \\ &\quad \left. + 2\xi^n \exp [I(\omega_x (i-1) + \omega_y j)] - \xi^n \exp [I(\omega_x (i-2) + \omega_y j)] \right) \\ &\quad - \frac{\Delta t}{(\Delta y)^3} \left(\xi^n \exp [I(\omega_x i + \omega_y (j+2))] - 2\xi^n \exp [I(\omega_x i + \omega_y (j+1))] \right. \\ &\quad \left. + 2\xi^n \exp [I(\omega_x i + \omega_y (j-1))] - \xi^n \exp [I(\omega_x i + \omega_y (j-2))] \right). \end{aligned} \quad (37)$$

By dividing both sides of Equation (37) with $\xi^n e^{I(\omega_x i + \omega_y j)}$, we have that

$$\begin{aligned} \xi^2 &= 1 - \frac{\Delta t}{(\Delta x)^3} \left(\xi \exp [2I\omega_x] - 2\xi \exp [I\omega_x] + 2\xi \exp [-I\omega_x] - \xi \exp [-2I\omega_x] \right) \\ &\quad - \frac{\Delta t}{(\Delta y)^3} \left(\xi \exp [2I\omega_y] - 2\xi \exp [I\omega_y] + 2\xi \exp [-I\omega_y] - \xi \exp [-2I\omega_y] \right). \end{aligned} \quad (38)$$

Equation (38) is equivalently given, using the trigonometric identity $\sin(\theta) = \frac{e^{I\theta} - e^{-I\theta}}{2I}$, as

$$\xi^2 = 1 - \frac{\Delta t}{(\Delta x)^3} \cdot \left(\xi \cdot I \cdot (2 \sin(2\omega_x) - 4 \sin(\omega_x)) \right) - \frac{\Delta t}{(\Delta y)^3} \cdot \left(\xi \cdot I \cdot (2 \sin(2\omega_y) - 4 \sin(\omega_y)) \right), \quad (39)$$

which simplifies to

$$\xi^2 + 2 \cdot \mathcal{B}(x, y) \cdot I \cdot \xi - 1 = 0, \quad (40)$$

where $\mathcal{B}(x, y) = r_x \cdot (\sin(\omega_x) - 2 \sin(\omega_x)) + r_y \cdot (\sin(2\omega_y) - 2 \sin(\omega_y))$, and r_x and r_y are given as in Equation (35). By solving the quadratic equation in Equation (40), we obtain

$$\xi = \frac{1}{2} \left(-2\mathcal{B}(x, y) \cdot I \pm \sqrt{4 - 4\mathcal{B}^2(x, y)} \right). \quad (41)$$

A condition for stability criterion is determined by finding a condition for $\Delta t, \Delta x$ so that for all θ, ξ an inequality $|\xi(\omega_x, \omega_y)| \leq 1$ is true; that is,

$$1 - \mathcal{B}^2(x, y) \geq 0 \implies |\mathcal{B}(x, y)| \leq 1. \quad (42)$$

Hence, Equation (42) is equivalently expressed as

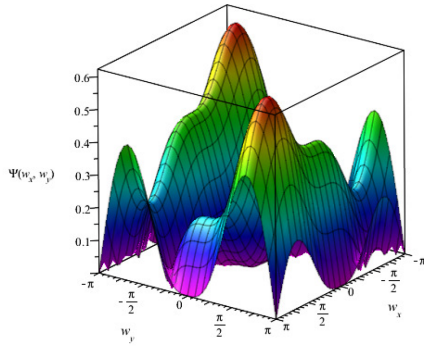
$$\left| r_x \cdot (\sin(2\omega_x) - 2\sin(\omega_x)) + r_y \cdot (\sin(2\omega_y) - 2\sin(\omega_y)) \right| \leq 1. \quad (43)$$

We fix $\Delta x = \Delta y = 0.1$. For stability, we need to solve

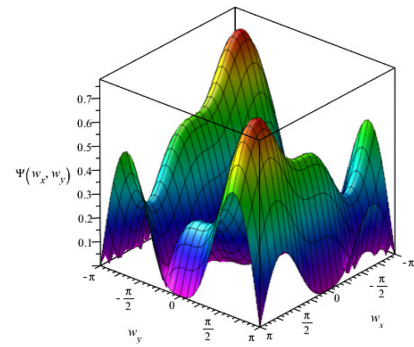
$$\left| \Psi(\omega_x, \omega_y, \Delta t) \right| \leq 1, \quad (44)$$

with $\Psi(\omega_x, \omega_y, \Delta t) := \frac{\Delta t}{(0.1)^3} \cdot (\sin(2\omega_x) - 2\sin(\omega_x)) + \frac{\Delta t}{(0.1)^3} \cdot (\sin(2\omega_y) - 2\sin(\omega_y))$.

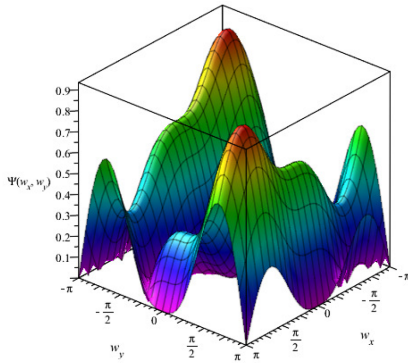
We use maple and deduce that stability region is $|\Delta t| \leq 0.00014$. We now give the 3D-graphical representation of $\Psi(\omega_x, \omega_y)$ vs Δt vs $\omega_x, \omega_y \in [-\pi, \pi]$ displayed as in Figure 8.



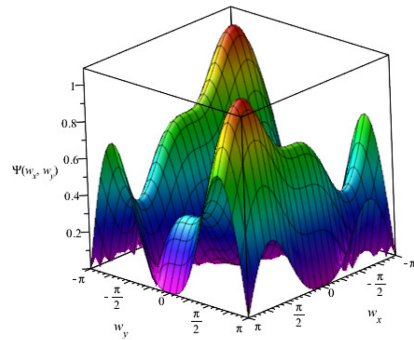
(a) Graph of Ψ vs ω_x vs ω_y for $\Delta t = 0.00010$ & $\Delta x = \Delta y = 0.1$



(b) Graph of Ψ vs ω_x vs ω_y for $\Delta t = 0.00012$ & $\Delta x = \Delta y = 0.1$



(c) Graph of Ψ vs ω_x vs ω_y for $\Delta t = 0.00014$ & $\Delta x = \Delta y = 0.1$



(d) Graph of Ψ vs ω_x vs ω_y for $\Delta t = 0.00016$ & $\Delta x = \Delta y = 0.1$

Figure 8: Graphs of Ψ vs ω_x vs ω_y for the Δt -values of $\Delta t = 0.00010, 0.00012, 0.00014, 0.00016$

Remark 5.2 *The above experimental simulation clearly shows that our numerical scheme in*

Equation (36) for the 2D dispersive KdV equation preserves stability for $\Delta t \leq 0.00014$ as depicted in the Figure 8, whereas the instability behavior emanates as shown in Figure 8d.

Let's consider the non-homogeneous 2D-dispersive equation as in Equation (3) with $(t, x, y) \in [0, T] \times \Omega$, $T > 0$, $\Omega = [0, 1] \times [0, 1]$, subject to the initial condition given in Equation (4) and the time-dependent non-zero boundary conditions in Equation (5).

We note here that the finite-difference scheme for Equation (3) works in such a way that the unknown value of $(i; j)$ at iteration $n + 1$; $U_{i,j}^{n+1}$ is computed at the preceding n^{th} -iteration values of the indices $(i + 1; j)$, $(i - 1; j)$, $(i - 2; j)$ $(i; j)$, $(i; j + 1)$, $(i; j - 1)$, and $(i; j - 2)$. The initial condition in Equation (4) tells us that $u(0, x, y) = u_{i,j}^1 = f(x_i, y_j)$ for $i = 1, 2, \dots, NP$, while the non-zero Dirichlet boundary conditions in Equation (5) gives the equations

$$\left. \begin{aligned} u(t_k, 0, y_j) &= u_{0,j}^k = \exp(t_k) \cos(x_i), & u(t_k, 1, y_j) &= u_{0,j}^k = \exp(t_k) \cos(1 + x_i) \\ u(t_k, x_i, 0) &= u_{i,0}^k = \cos(x_i + 2t_k), & u(t_k, x_i, 1) &= u_{i,0}^k = \cos(x_i + 1 + 2t_k) \end{aligned} \right\} \quad (45)$$

for $i, j \in \{1, 2, \dots, NP\}$. In other words, if (x_i, y_j) is a boundary node, then $u_{i,j}^n = g(x_i, y_j, t_k)$ where g is considered from the non-zero Dirichlet boundary conditions given in (5).

We now give some results for Equation (3) and 3D-graphical representation of the solution using classical finite-difference scheme obtained at times $t = 0.1, 1.0, 2.0$.

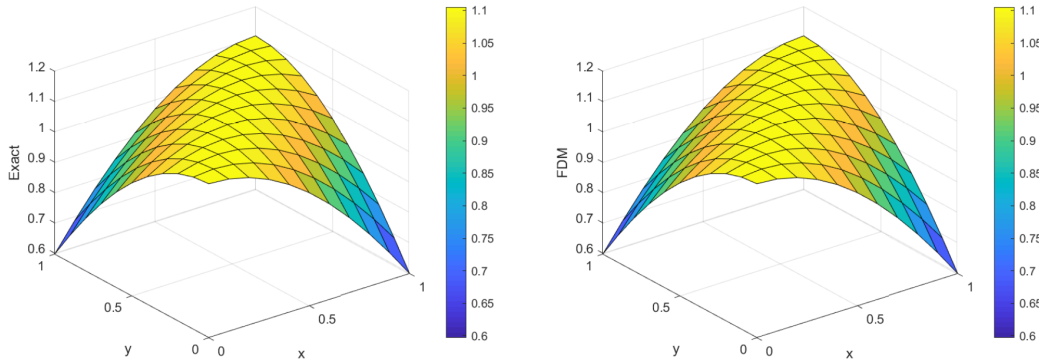


Figure 9: Graphs of numerical FDM solution for Equation (3) for $(x; y) \in \Omega$, $\Omega = (0, 1)^2$ ($\Delta t = 10^{-4}$) at times $t = 0.1$

Tables 7 - 9 show the exact and numerical solution using FDM together with the absolute and relative errors at some mesh points of the 2D KdV equation as given in Equation (3).

Table 7: A comparison between the exact solution and FDM solution at some values of x and y at time $t = 0.1$

t	x	y	Exact	FDM	Absolute error	Relative error
0.0	0.0	0.0	1.105171	1.105171	0.000000	0.000000
0.2	0.2	0.2	1.105171	1.105171	3.272759×10^{-9}	2.961315×10^{-9}
		0.4	1.083141	1.083141	1.980772×10^{-9}	1.828729×10^{-9}
		0.6	1.017929	1.017929	2.657259×10^{-9}	2.610454×10^{-9}
		0.8	9.121369×10^{-1}	9.121369×10^{-1}	1.202890×10^{-10}	1.318760×10^{-10}
0.10	0.4	0.2	1.083141	1.083141	1.980772×10^{-9}	1.828729×10^{-9}
		0.4	1.105171	1.105171	1.898155×10^{-10}	1.717522×10^{-10}
		0.6	1.083141	1.083141	2.864586×10^{-10}	2.644703×10^{-10}
		0.8	1.017929	1.017929	2.278236×10^{-9}	2.238107×10^{-9}
0.6	0.2	0.2	1.017929	1.017930	2.657260×10^{-9}	2.610455×10^{-9}
		0.4	1.083141	1.083141	2.864542×10^{-10}	2.644662×10^{-10}
		0.6	1.105171	1.105171	7.864502×10^{-10}	7.116096×10^{-10}
		0.8	1.083141	1.083141	1.605691×10^{-9}	1.482439×10^{-9}
0.8	0.2	0.2	9.121377×10^{-1}	9.121369×10^{-1}	1.202870×10^{-10}	1.318738×10^{-10}
		0.4	1.017930	1.017929	2.278236×10^{-9}	2.238107×10^{-9}
		0.6	1.083141	1.083141	1.605688×10^{-9}	1.482437×10^{-9}
		0.8	1.105171	1.105171	2.971336×10^{-9}	2.688576×10^{-9}
1.0	1.0	1.105171	1.105171	0.000000	0.000000	

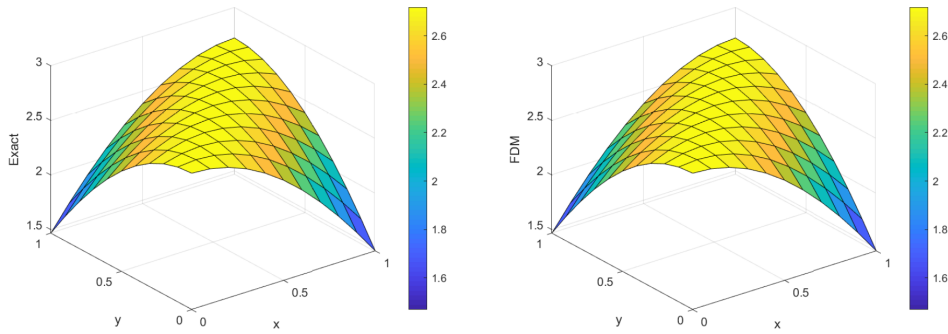


Figure 10: Graphs of numerical FDM solution for Equation (3) for $(x; y) \in \Omega$, $\Omega = (0, 1)^2$ ($\Delta t = 10^{-4}$) at times $t = 1.0$

Table 8: A comparison between the exact solution and FDM solution at some values of x and y at time $t = 1.0$.

t	x	y	Exact	FDM	Absolute error	Relative error
0.0	0.0	0.0	2.718282	2.718282	0.000000	0.000000
0.2	0.2	0.2	2.718282	2.718282	1.049272×10^{-9}	3.860057×10^{-10}
		0.4	2.664097	2.664097	2.49956×10^{-9}	9.382401×10^{-10}
		0.6	2.503703	2.503703	1.876913×10^{-9}	7.496546×10^{-10}
		0.8	2.243495	2.243498	1.960433×10^{-9}	8.738300×10^{-10}
1.0	0.4	0.2	2.664097	2.664097	2.499576×10^{-9}	9.382449×10^{-10}
		0.4	2.718282	2.718282	6.650187×10^{-9}	2.446467×10^{-9}
		0.6	2.664097	2.664097	4.694272×10^{-9}	1.762049×10^{-9}
		0.8	2.503703	2.503703	4.319871×10^{-9}	1.725393×10^{-9}
0.6	0.2	0.2	2.503703	2.503703	1.876908×10^{-9}	7.496529×10^{-10}
		0.4	2.664097	2.664097	4.694277×10^{-9}	1.762052×10^{-9}
		0.6	2.718282	2.718282	3.124026×10^{-9}	1.149265×10^{-9}
		0.8	2.664097	2.664097	3.635947×10^{-9}	1.364795×10^{-9}
0.8	0.2	0.2	2.243495	2.243495	1.960426×10^{-9}	$8.7382687 \times 10^{-10}$
		0.4	2.503703	2.503703	4.319886×10^{-9}	1.725398×10^{-9}
		0.6	2.664097	2.664097	3.635933×10^{-9}	1.364789×10^{-9}
		0.8	2.718282	2.718282	3.871336×10^{-9}	1.424185×10^{-9}
1.0	1.0	2.718282	2.718282	0.000000	0.000000	

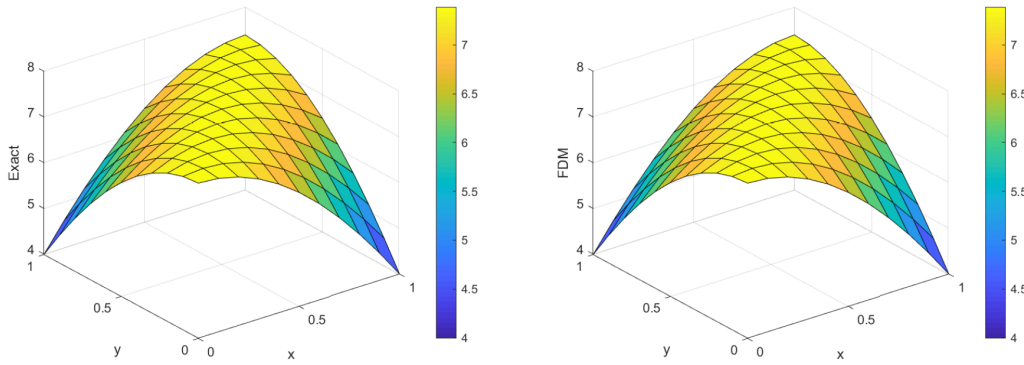
Figure 11: Graphs of numerical FDM solution for Equation (3) for $(x; y) \in \Omega$, $\Omega = (0, 1)^2$ ($\Delta t = 10^{-4}$) at times $t = 2.0$

Table 9: A comparison between the exact solution and FDM solution at some values of x and y at time $t = 2.0$

t	x	y	Exact	FDM	Absolute error	Relative error
0.0	0.0	0.0	7.389056	7.389056	0.000000	0.000000
0.2	0.2	0.2	7.389056	7.389056	6.118424×10^{-9}	8.280386×10^{-10}
		0.4	7.241767	7.241767	9.911319×10^{-9}	1.368633×10^{-9}
		0.6	6.805771	6.805771	9.219519×10^{-9}	1.354662×10^{-9}
		0.8	6.098451	6.098451	7.290955×10^{-9}	1.195542×10^{-9}
2.0	0.4	0.2	7.241767	7.241767	9.911327×10^{-9}	1.368634×10^{-9}
		0.4	7.389056	7.389056	1.911231×10^{-8}	2.586569×10^{-9}
		0.6	7.241767	7.241767	1.745360×10^{-8}	2.410131×10^{-9}
		0.8	6.805771	6.805771	1.382399×10^{-8}	2.031217×10^{-9}
0.6	0.2	0.2	6.805771	6.805771	9.219479×10^{-9}	1.354656×10^{-9}
		0.4	7.241767	7.241767	1.745363×10^{-8}	2.410134×10^{-9}
		0.6	7.389056	7.389056	1.7229377×10^{-8}	2.331743×10^{-9}
		0.8	7.241767	7.241767	1.290448×10^{-8}	1.781952×10^{-9}
0.8	0.2	0.2	6.098451	6.098451	7.290940×10^{-9}	1.195540×10^{-9}
		0.4	6.805771	6.8057713	1.382399×10^{-8}	2.031217×10^{-9}
		0.6	7.241767	7.241767	1.290455×10^{-8}	1.781962×10^{-9}
		0.8	7.389056	7.389056	1.218181×10^{-8}	1.648628×10^{-9}
1.0	1.0	7.389056	7.389056	0.000000	0.000000	

6. Discussion and Conclusions

In this paper, we have solved one-dimensional homogeneous and two-dimensional non-homogeneous dispersive KdV-type equations by employing two reliable methods namely the reduced differential transform method and the classical finite difference method. The absolute and relative errors are very small, as shown in the tables, therefore the current approaches offer great accuracy for the numerical solutions of the considered experiments.

From comparison tables, the results obtained by using the classical finite difference method are better, for longer propagation times, than those obtained from RDTM and some other semi-numerical schemes such as Adomian decomposition and Homotopy perturbation methods, these may be due to some computation of Adomian polynomials [4, 5], and He's polynomials [14, 15].

The first numerical experiment comprised a homogeneous third-order KdV equation. RDTM is very effective at small propagation time ($t = 0.01, 0.05$) giving relative error of order 10^{-8} , 10^{-4} , but less effective at medium propagation time ($t = 0.10, 0.125$) giving relative error of 10^{-2} . The classical finite difference method is very efficient at small, medium and long propagation times ($t = 0.01, 0.05, 1.0$), with relative error of order 10^{-7} to 10^{-6} .

The second numerical experiment consisted of non-homogeneous 2D-linearized dispersive KdV equation. Our findings indicate that RDTM perform better than the classical FDM for short propagation times, say, at $t = 0.1$ as shown in Table 3 and the corresponding relative error at this time is of order 10^{-16} . While the classical FDM defeats RDTM for medium and long propagation times; i.e., when $t = 1.0$ and $t = 4.0$ as the relative error using FDM at times $t = 1.0$ and $t = 2.0$ are of order 10^{-10} and 10^{-9} , respectively. This study not only shows RDTM gives an approximate-

analytical exact solution for Equation (3), but also the classical FDM is a more reliable method for large propagation times.

A clear conclusion can be drawn from the numerical results for the considered experiments in the sense that RDTM and FDM algorithms provide highly accurate numerical solutions for the considered KdV equations. It is also worth noting that the advantage of the approximation of the series methodologies such as RDTM shows a quick convergence of the solutions. Besides, RDTM does not require much information about the boundary conditions of the given problems. The initial condition is used, but the boundary conditions may not always have to be specified and it also does not require linearization, discretization or perturbation. To apply the classical FDM to the given problems, we have primarily checked the von Neumann criterion and we have found reliable numerical results for the considered experiments. The study confirms the significance of the comparison between semi-analytical and numerical methods for solving some dispersive KdV-type PDEs.

Therefore, the obtained results from the study reveal the complete reliability of the employed methods with great potential in scientific applications to handle numerous complicated linear and nonlinear problems.

Acknowledgments

Abey S. Kelil was supported by NMU Council postdoctoral fellowship (March 2020 to February 2022). He also gratefully acknowledges top-up funding from CoE-MaSS for the period January 2021 to December 2021.

Declaration of Ethical Standards

The author declares that the materials and methods used in their study do not require ethical committee and/or legal special permission.

Conflict of Interest

The author declares no conflicts of interest.

References

- [1] Abassy T.A., El-Tawil M.A., Saleh H.K., *The solution of KdV and mKdV equations using Adomian Padé approximation*, International Journal of Nonlinear Sciences and Numerical Simulation, 5(4), 327-339, 2004.
- [2] Abassy T.A., El-Tawil M.A., El Zoheiry H., *Toward a modified variational iteration method*, Journal of Computational and Applied Mathematics, 207(1), 137-147, 2007.
- [3] Aderogba A.A., Appadu A.R., *Classical and multisymplectic schemes for linearized KdV equation: Numerical results and dispersion analysis*, Fluids, 6(6), 214, 2021.
- [4] Adomian G., *Solving Frontier Problems of Physics: The Decomposition Method*, Kluwer Academic Publishers, 1994.

- [5] Adomian G., *A review of decomposition method and some recent results for nonlinear equation*, Mathematical and Computer Modelling, 13(7), 17-43, 1992.
- [6] Adomian G., Rach R., *Noise terms in decomposition solution series*, Applied Mathematics and Computation, 24(11), 61-64, 1992.
- [7] Al-Amr M.O., *New applications of reduced differential transform method*, Alexandria Engineering Journal, 53, 243-247, 2014.
- [8] Appadu A.R., Kelil A.S., *On semi-analytical solutions for linearized dispersive KdV equation*, Mathematics, 8(10), 1769, 2020.
- [9] Appadu A.R., Chapwanya M., Jejenywa O.A., *Some optimised schemes for 1D Korteweg-de-Vries equation*, Progress in Computational Fluid Dynamics, 17(4), 250-266, 2017.
- [10] Appadu, A.R., Kelil, A.S., *Comparison of modified ADM and classical finite difference method for some third-order and fifth-order KdV equations*, Demonstratio Mathematica, 54(1), 377-409, 2021.
- [11] Ascher U.M., Numerical Methods for Evolutionary Differential Equations, Society for Industrial and Applied Mathematics, 2008.
- [12] Chen S.S., Chen C.K., *Application to differential transformation method for solving systems of differential equations*, Nonlinear Analysis Real World Applications, 10, 881-888, 2009.
- [13] He J.H., *Homotopy perturbation technique*, Computer Methods in Applied Mechanics and Engineering, 178, 257-262, 1999.
- [14] He J.H., *Homotopy perturbation method: A new non-linear analytical technique*, Applied Mathematics and Computation, 135, 73-79, 2003.
- [15] He J.H., *Application of homotopy perturbation method to nonlinear wave equations*, Chaos, Solitons and Fractals, 26, 695-700, 2005.
- [16] He J.H., *Variational iteration method—a kind of non-linear analytical technique: Some examples*, International Journal of Non-Linear Mechanics, 34(4), 699-708, 1999.
- [17] He J.H., *A new approach to nonlinear partial differential equations*, Communications in Nonlinear Science and Numerical Simulation, 2(4), 230-235, 1997.
- [18] Keskin Y., Oturanc G., *Reduced differential transform method for partial differential equations*, International Journal of Nonlinear Sciences and Numerical Simulation, 10(6), 741-750, 2009.
- [19] Keskin Y., Oturanc G., *Reduced differential transform method for solving linear and nonlinear wave equations*, Iranian Journal of Science and Technology, Transaction A, 34(A2), 113-122, 2010.
- [20] Korteweg D.J., de Vries G., *On the change of form of long waves advancing in a rectangular canal, and on a new type of long stationary waves*, Philosophical Magazine, 39, 422-443, 1895.
- [21] Taha T.R., Ablowitz M.I., *Analytical and numerical aspects of certain nonlinear evolution equations III: Numerical, Korteweg-de Vries equation*, Journal of Computational Physics, 55(2), 231-253, 1984.
- [22] Wazwaz A.M., *An analytic study on the third-order dispersive partial differential equations*, Applied Mathematics and Computation, 142(2-3), 511-520, 2003.
- [23] Yildirim A., *On the solution of the nonlinear Korteweg-de Vries equation by the homotopy perturbation method*, Communications in Numerical Methods in Engineering, 25(12), 1127-1136, 2009.
- [24] Zabusky N.J., Kruskal M.D., *Interaction of “solitons” in a collisionless plasma and the recurrence of initial states*, Physical Review Letters, 15(6), 240, 1965.

- [25] Zhou J.K., Differential Transformation and Its Applications for Electrical Circuits, Huazhong University Press, 1986.